Journal of Solid State Chemistry 186 (2012) 204–207

Contents lists available at SciVerse ScienceDirect

Journal of Solid State Chemistry

journal homepage: www.elsevier.com/locate/jssc

Structure–composition–luminescence correlations in $Sr_{2.5-3x/2}Ba_{0.5}Sm_xAl_{1-y}In_yO_4F$ ($0.001 \le x, y \le 0.1$) oxyfluorides

Sangmoon Park*

Department of Engineering in Energy & Applied Chemistry, Silla University, Busan 617-736, Republic of Korea

ARTICLE INFO

Article history:
Received 29 July 2011
Received in revised form
22 October 2011
Accepted 11 December 2011
Available online 17 December 2011

Keywords:
Photoluminescence
Oxyfluorides
Sm^{3+} transitions
Phosphor

ABSTRACT

Luminescent materials composed of $Sr_{2.5-3x/2}Ba_{0.5}Sm_xAl_{1-y}In_yO_4F$ ($0.001 \le x, y \le 0.1$) were prepared by the solid-state reaction method. After the replacement of Sr^{2+} and Al^{3+} ions by Sm^{3+} and In^{3+} ions in $Sr_{2.5}Ba_{0.5}AlO_4F$ host structure, a novel charge-transfer band centered around 304 nm shifted from 240 nm is monitored; moreover, sharp and well-resolved emission peaks in the $^4G_{5/2} \rightarrow {}^6H_J$ transitions of the Sm^{3+} activator are observed. The diverse excitation and emission photoluminescence spectra of $Sr_{2.5-3x/2}Ba_{0.5}Sm_xAl_{1-y}In_yO_{4-\alpha}F_{1-\delta}$ ($0.001 \le x, y \le 0.1$) phosphors originated by the charge-transfer of the host to the Sm^{3+} activator, the *f–f* transitions in the Sm^{3+} ions, and the defect-induced self-activation are also introduced.

1. Introduction

Highly energy-efficient light emitting diodes (LEDs) are finding use in many areas, such as industrial and domestic illumination, indicator lights, pedestrian and traffic signs, automotive dashboards, video displays, backlight units, and planting and medical light sources [1].

Among the several techniques for the production of LED-chip-based or LED-chip-plus-phosphor-based white light sources, three are the most widely used [1,2]. The first of these is based on combining red, green, and blue LED chips to emit white light. The second is based on the combination of a blue LED chip with a yellow phosphor. Cerium-doped yttrium–aluminum–garnet (YAG) is the most prevalent yellow phosphor which is excited by blue light from an InGaN LED chip emitting near 465 nm. However, it has low color rendering of white LEDs due to the moderately weak emission in the red spectral region, so light parameters of white LED could be gradually adjusted by co-doping Sm^{3+} with Ce^{3+} in YAG to enhance red emission [2]. The last technique is based on combining UV LED chips with red, green, and blue colored phosphors or a single-phased white-emitting phosphor. $Y_2O_2S:Eu^{3+}$, $ZnS:Cu^+,Al^{3+}$, and $BaMgAl_{10}O_{17}:Eu^{2+}$ could be used as the red-, green-, and blue-emitting phosphors, respectively. $Ba_3MgSi_2O_8:Eu^{2+}$, Mn^{2+} and $SrZn_2(PO_4)_2:Eu^{2+}$, Mn^{2+} are typical examples of single-phased white-emitting phosphors, which are favored over UV LED [3,4]. To improve the high color rendering and stable color point in near-UV LED applications, the combination of red activators Eu^{3+} and Sm^{3+} can be widely exploited [2,5]. These red-emitting phosphors could be enhanced by the significant energy transfer from Sm^{3+} to Eu^{3+} due to the increase in absorption efficiency. Sm^{3+}-activated phosphors are usually excited by charge transfer from the host lattice to the activator and the *f–f* transitions of the activator. The insufficient absorption strength of the charge transfer state and the low cross section of the *f–f* transitions of Sm^{3+} ions in the near-UV or visible range has limited the use of Sm^{3+}-activated luminescent materials [6].

$Sr_{3-x}A_xAl_{1-y}In_yO_{4-\alpha}F_{1-\delta}$ (A=Ca, Ba and $0 \le x \le 1$ and $0 \le y \le 0.1$) and Eu^{3+}-doped $Sr_{3-x}A_xAl_{1-y}In_yO_{4-\alpha}F_{1-\delta}$ phosphors were previously introduced [7,8]. Exciting the phosphors with near-UV light near 365 nm revealed broad-band photoluminescence (PL) emission due to the self-activation of the oxyfluoride host lattice by defects created using appropriate post-synthesis reduction conditions. In this paper, the structure–composition–luminescence relationships in $Sr_{2.5-3x/2}Ba_{0.5}Sm_xAl_{1-y}In_yO_4F$ ($0.001 \le x, y \le 0.1$) phosphors are discussed. When replacing Sr^{2+} and Al^{3+} ions in the oxyfluoride host by Sm^{3+} and In^{3+} ions, respectively, the effective charge-transfer band (CTB) and *f–f* transitions of Sm^{3+} ions were monitored. The characterized excitation and emission PL spectra of the defect-induced $Sr_{2.5-3x/2}Ba_{0.5}Sm_xAl_{1-y}In_yO_{4-\alpha}F_{1-\delta}$ phosphors were also attained.

2. Experimental

Samples of $Sr_{2.5-3x/2}Ba_{0.5}Sm_xAl_{1-y}In_yO_4F$ ($0.001 \le x, y \le 0.1$) were prepared by heating the appropriate stoichiometric amounts of $SrCO_3$ (Aldrich 99.9%), $BaCO_3$ (Alfa, 99.95%), SrF_2 (Aldrich 99.99%), Al_2O_3 (Alfa 99.95%), In_2O_3 (Alfa 99.9%), and Sm_2O_3 (Alfa 99.9%) at temperatures up to 1050 °C for 3 h in air. The

* Fax: +82 51 999 5335.
E-mail address: spark@silla.ac.kr

0022-4596/$ - see front matter © 2011 Elsevier Inc. All rights reserved.
doi:10.1016/j.jssc.2011.12.014

as-made $Sr_{2.5-3x/2}Ba_{0.5}Sm_xAl_{1-y}In_yO_4F$ ($0.001 \le x,\ y \le 0.1$) samples were subsequently annealed for 1 h at 900 °C in reducing atmosphere (5% H_2/95% Ar) to synthesize self-activating luminescent materials. Phase identification of phosphors was done using a Shimadzu XRD-6000 powder diffractometer using Cu$K\alpha$-radiation, and the unit cell parameters were determined by using the least squares refinement program CELREF. Ultraviolet–visible spectroscopy and a spectrofluorometer (Sinco Fluromate FS-2) was used to measure the excitation and emission spectra of the $Sr_{2.5-3x/2}Ba_{0.5}Sm_xAl_{1-y}In_yO_4F$ and $Sr_{2.5-3x/2}Ba_{0.5}Sm_xAl_{1-y}In_yO_{4-\alpha}F_{1-\delta}$ ($0.001 \le x,\ y \le 0.1$) phosphor materials.

3. Results and discussion

The anion-ordered Sr_3AlO_4F oxyfluoride structure, a tetragonal phase with space group *I*4/*mcm*, was well elucidated as an efficient luminescent host material activated under UV and near-UV regions in a previous report [9]. As shown in Fig. 1, the host lattice is arranged by stacking alternating $Sr(2)_2F^{3+}$ and $Sr(1)AlO_4^{3-}$ layers along the *c* axis. Sr(2) ions, and AlO_4 tetrahedra are located in the $Sr(1)AlO_4^{3-}$ layer in a checkerboard arrangement. This oxyfluoride host can be alternatively described as an ABX_3 antiperovskite structure, where the AlO_4^{5-}, F^-, and Sr^{2+} ions occupy the *A* site, octahedral *B* site, and the bridging *X* site, respectively [10]. There are tenfold coordinated Sr(1) and eightfold coordinated Sr(2) cation sites; moreover, the oxyfluoride host lattice consists of both strong ionic Sr–F and covalent Al–O bonds. For the study of the structure–composition–luminescence relationships in oxyfluoride phosphors, the luminescent host lattice was simply fixed to the $Sr_{2.5}Ba_{0.5}$ AlO_4F composition. Sr^{2+} and Al^{3+} ions are replaced by Sm^{3+} and In^{3+} ions, respectively, for their correlations in the oxyfluoride host lattice.

Fig. 2(a) depicts the X-ray diffraction (XRD) pattern of the calculated Sr_3AlO_4F (ICSD 50736) with lattice parameters $a=6.78(1)$ and $c=11.14(1)$ Å. The XRD patterns of $Sr_{2.35}Ba_{0.5}$ $Sm_{0.1}AlO_4F$ and $Sr_{2.35}Ba_{0.5}Sm_{0.1}Al_{0.9}In_{0.1}O_4F$ oxyfluoride phosphors in Fig. 2(b) and (c) show the single-phase host lattice without any obvious impurities indexed in a tetragonal unit cell. Partial substitution of Sr^{2+} ($r=1.36$ Å for 10 CN, $r=1.26$ Å for 8 CN) ions by 0.5 mol Ba^{2+} ($r=1.52$ Å for 10 CN) and 0.1 mol Sm^{3+} ($r=1.079$ Å for 8 CN) ions in the $Sr_{2.35}Ba_{0.5}Sm_{0.1}AlO_4F$ oxyfluoride host resulted in a significant shift to lower angles as the cell size increased to $a=6.82(1)$ and $c=11.143(2)$ Å [11,12]. As discussed previously, the larger Ba^{2+} and smaller Sm^{3+} ions could suitably be occupied in tenfold coordinated Sr(1) and eightfold coordinated Sr(2) sites, respectively. There is a gradual shift in the positions of the various Bragg reflections to lower angles for $Sr_{2.35}Ba_{0.5}Sm_{0.1}Al_{0.9}In_{0.1}O_4F$ ($a=6.831(3)$ and $c=11.190(1)$ Å) upon addition of the larger In^{3+} ion ($r=0.62$ Å for 4 CN) to the Al^{3+} ($r=0.39$ Å for 4 CN) site. After the replacement of the light-metal Al^{3+} by the heavy-metal ions In^{3+} in $Sr_{2.35}Ba_{0.5}Sm_{0.1}AlO_4F$, the luminescent

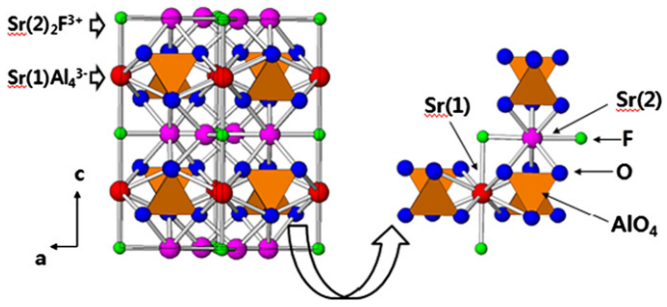

Fig. 1. Crystallographic structure of Sr_3AlO_4F oxyfluoride host lattice.

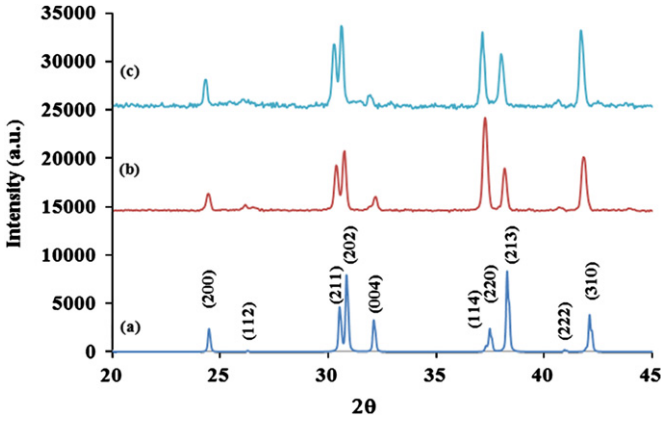

Fig. 2. X-ray diffraction patterns of (a) the calculated Sr_3AlO_4F and the observed (b) $Sr_{2.35}Ba_{0.5}Sm_{0.1}AlO_4F$ and (c) $Sr_{2.35}Ba_{0.5}Sm_{0.1}Al_{0.9}In_{0.1}O_4F$ phosphors.

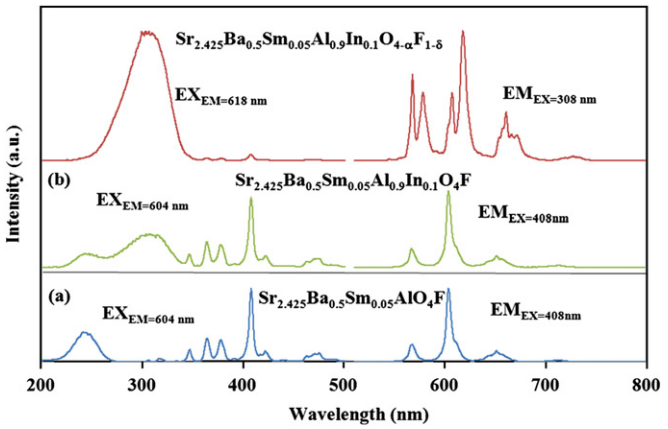

Fig. 3. The excitation and emission spectra of (a) $Sr_{2.425}Ba_{0.5}Sm_{0.05}AlO_4F$ and (b) $Sr_{2.425}Ba_{0.5}Sm_{0.05}Al_{0.9}$ $In_{0.1}O_4$ F (bottom) and $Sr_{2.425}Ba_{0.5}Sm_{0.05}Al_{0.9}$ $In_{0.1}O_{4-\alpha}F_{1-\delta}$ (top) luminescent materials.

host lattice was incited by the increase in covalency due to the presence of heavy metal ions, which facilitated the electronic carrier transfer.

When the Sm^{3+} content reached $x=0.05$ (5 mol%) in the $Sr_{2.5-3x/2}Ba_{0.5}Sm_xAlO_4F$ phosphors, the relative luminescent intensity clearly reached the maximum [11]. Furthermore, the orange emission of the first region in the PL spectra reveals a broad excitation band around 240 nm caused by the charge-transfer transition from the host to the Sm^{3+} ions, and the other region is attributed to the large intense *f*–*f* transitions of the Sm^{3+} ions that ranged broadly from 290 to 480 nm in Fig. 3(a). The strongest excitation peak in the $Sr_{2.425}Ba_{0.5}Sm_{0.05}AlO_4F$ PL spectra located near 408 nm is attributed to the $^6H_{5/2} \rightarrow {}^4L_{13/2}$ transition of Sm^{3+} ions. Under the excitation of 408 nm, there is a sharp and prominent orange emission peak in the $S_{2.425}Ba_{0.5}Sm_{0.05}AlO_4F$ phosphor that corresponds to the $^4G_{5/2} \rightarrow {}^6H_{7/2}$ transition of Sm^{3+} at 604 nm alongside the three relatively weak peaks assigned to the $^4G_{5/2} \rightarrow {}^6H_{5/2}$ (565 nm), $^4G_{5/2} \rightarrow {}^6H_{9/2}$ (644 nm), and $^4G_{5/2} \rightarrow {}^6H_{11/2}$ (707 nm). It is known that the *f*–*f* transitions of Sm^{3+} ions produced by electric-dipoles and magnetic-dipoles generate the desirable orange emission. Tamura et. al. classified the Sm^{3+}-activated emission spectra into two regions: the first two emission lines ($^4G_{5/2} \rightarrow {}^6H_{5/2}$, $^4G_{5/2} \rightarrow {}^6H_{7/2}$) are allowed by both electric-dipole and magnetic-dipole transitions, whereas the third line ($^4G_{5/2} \rightarrow {}^6H_{9/2}$) is only allowed by electric-dipole transitions [13,14]. It was reported that the crystal field effect on the emission intensity at the third line (644 nm) is larger than that

at the first two lines (565, 604 nm); however, the emission intensity at the third line is weak when the Sm^{3+} ions are in the symmetric site that possesses an inversion center, as shown in Fig. 1. When the Al^{3+} ions are replaced by In^{3+} ions in $S_{2.425}Ba_{0.5}Sm_{0.05}AlO_4F$, the PL spectrum is attributed to the new CTB centered around 304 nm under the 603 nm light shown in Fig. 3(b) (bottom). Exceptionally strong excitation and emission spectra in $S_{2.425}Ba_{0.5}Sm_{0.05}Al_{0.9}In_{0.1}O_{4-\alpha}F_{1-\delta}$ phosphors were observed under the 618 and 304 nm light, as shown in Fig. 3(b) (top). In Fig. 3(b), the excitation spectrum with a broad band centered at 304 nm can be assigned to the CTB attributed to In^{3+}–O^{2-} charge transfer. The substitution of the larger In^{3+} cations in the Al^{3+} site causes strong covalency, lowering the chemical bonding energy in the oxyfluoride host lattice. Fig. 3(b) (top) shows the weak *f–f* transitions of the Sm^{3+} ions through 480 nm light that are caused by the parity forbidden nature of the *f–f* transitions [15]. Novel, sharp, and well-resolved emission lines can be observed in Fig. 3(b) (top). The crystal-field effect on the transitions of Sm^{3+} in the oxyfluoride host lattices is the cause of the strong splitting emission peaks. The partial substitution of the InO_4 tetrahedra in $S_{2.425}Ba_{0.5}Sm_{0.05}AlO_4F$ oxyfluoride structure formulates more a favorable local distortion and drives the Sm^{3+} ions into the distorted Sr(2) site. Sakirzanovas et al. [6] have reported that the emission spectra represented well-split $^4G_{5/2}\rightarrow{}^6H_J$ transitions in Sm^{3+}-doped borate compounds owing to the strong crystal-field effect. 4*f* electrons of rare-earth ions in solids are commonly not very sensitive to the effect of the surrounding crystal field because of the outer shell shielding; however, the PL emission spectra can be affected by the Stark effect caused by the crystal-field effect. Furthermore, the unpaired electrons in the partially filled $4f^5$ electrons of the Sm^{3+} ions in a fine host lattice can generate twice the Kramer degeneration in any crystal field lower than cubic [6]. The plot of the relative intensity as a function of different Sm^{3+} (x) and In^{3+} (y) contents in $Sr_{2.5-3x/2}Ba_{0.5}$ $Sm_xAl_{1-y}In_yO_4F$ ($0.001\le x, y\le 0.1$) phosphors is shown in Fig. 4. The excitation spectra centered at 240 nm as well as the emission spectra maximized at 603 nm were observed in $Sr_{2.5-3x/2}Ba_{0.5}$ $Sm_xAl_{1-y}In_yO_4F$ ($x, y=0.001$ and $x=0.001$, $y=0.01$) phosphors. New CTB centered at 308 nm and well-split emission peaks maximized at 618 nm become visible when the oxyfluoride host composition is $x=0.001$ and $y=0.05$. The intensity of CTB dramatically increased with Sm^{3+} and In^{3+} content in the oxyfluoride phosphors. The intensity of the excitation spectra derived by the *f–f* transition of the Sm^{3+} ions at 408 nm does not primarily depend on the increase of the In^{3+} concentration. However, when Sm^{3+} ions are added in the host lattice, the strong *f–f* transition of Sm^{3+} at 408 nm and the emission peaks maximized at 603 nm are manifestly increased. As concentration quenching was exhibited for Sm^{3+} contents in excess of 5% in the $Sr_{2.5-3x/2}Ba_{0.5}$ Sm_xAlO_4F oxyfluoride host [11], the preference of the relative emission intensity at 603 nm under

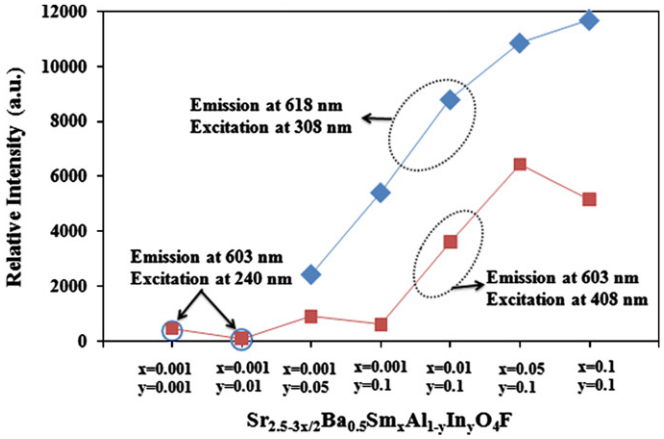

Fig. 4. The relative intensity as a function of Sm^{3+} (x) and In^{3+} (y) contents in $Sr_{2.5-3x/2}Ba_{0.5}$ $Sm_xAl_{1-y}In_yO_4F$ ($0.001\le x, y\le 0.1$) phosphors.

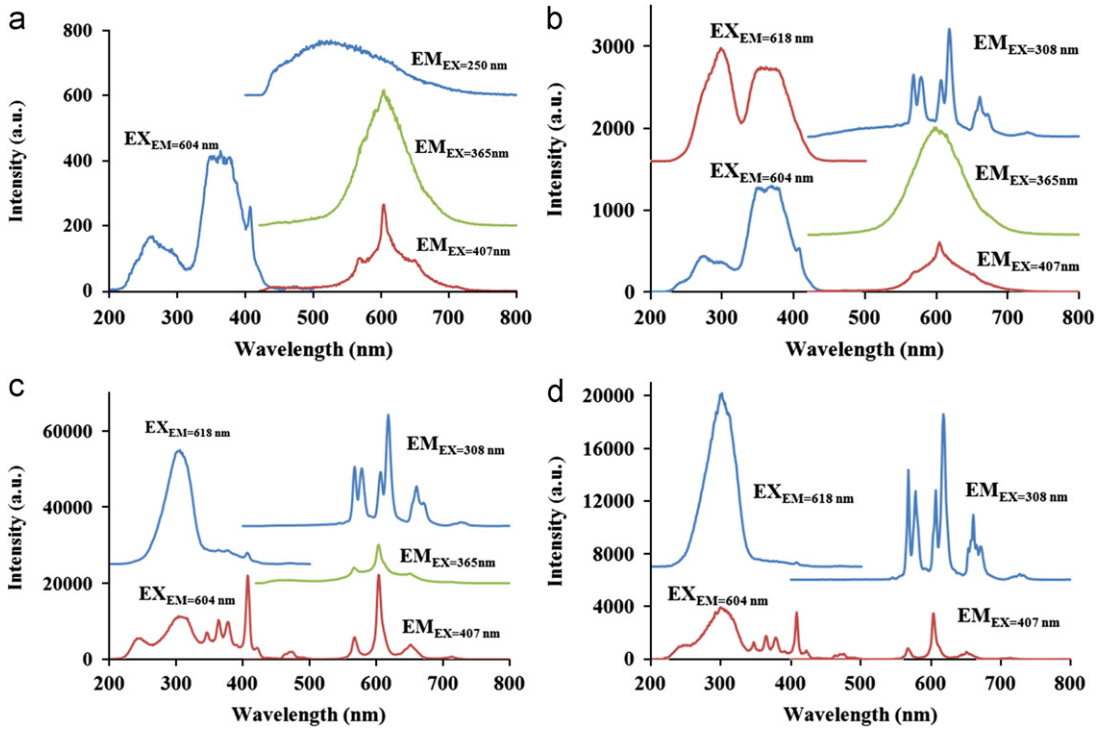

Fig. 5. The excitation and emission spectra of defect-induced $Sr_{2.5-3x/2}Ba_{0.5}$ $Sm_xAl_{1-y}In_yO_{4-\alpha}F_{1-\delta}$ phosphors (a) $x=0.001$, $y=0.01$, (b) $x=0.001$, $y=0.1$, (c) $x=0.05$, $y=0.1$, and (d) $x=0.1$, $y=0.1$.

the excitation of 408 nm in $Sr_{2.5-3x/2}Ba_{0.5}$ $Sm_xAl_{1-y}In_yO_4F$ was also monitored.

The PL excitation and emission spectra of the defect-induced $Sr_{2.5-3x/2}Ba_{0.5}Sm_xAl_{1-y}In_yO_{4-\alpha}F_{1-\delta}$ phosphors are depicted in Fig. 5, where (a) $x=0.001$, $y=0.01$, (b) $x=0.001$, $y=0.1$, (c) $x=0.05$, $y=0.1$, and (d) $x=0.1$, $y=0.1$. These defect-induced $Sr_{2.5-3x/2}Ba_{0.5}$ $Sm_xAl_{1-y}In_yO_{4-\alpha}F_{1-\delta}$ oxyfluoride phosphors were prepared by exposing $Sr_{2.5-3x/2}Ba_{0.5}$ $Sm_xAl_{1-y}In_yO_4F$ to a 5%H_2/95%Ar atmosphere at 900 °C for 1 h. The characteristic excitation spectrum centered at 250, 365, and 407 nm under 604 nm light ($EX_{EM=604\ nm}$) was monitored. The self-activated band emission under the excitation of 250 nm ($EM_{EX=250\ nm}$) was provided by the defect-induced oxyfluoride host lattice at low concentration of Sm^{3+} and In^{3+} ions [11]. In accordance with what was reported in a previous study [8], a significant intensity was obtained in the excitation spectrum centered at 365 nm and the broad-band PL emission centered at 600 nm ($EM_{EX=365\ nm}$) due to self-activation in the oxyfluoride lattice by substituting In^{3+} ions into the Al^{3+} positions. The sharp excitation light of 407 nm clearly generates the line emission ($EM_{EX=407\ nm}$) from the Sm^{3+} transitions together with the band emission derived from self-activation in the $Sr_{2.5}Ba_{0.5}Al_{1-y}In_yO_{4-\alpha}F_{1-\delta}$ host lattice. In contrast to Fig. 5(a), a new CTB centered 308 nm was especially apparent when the contents of the Sm^{3+} and In^{3+} ions reached $x=0.001$ and $y=0.1$ in the $Sr_{2.5}Ba_{0.5}Al_{1-y}In_yO_{4-\alpha}F_{1-\delta}$ host lattice, as shown in Fig. 5(b). Furthermore, sharp splitting emission peaks from the Sm^{3+} transitions are clearly present whereas the self-activated band emission under the excitation of 250 nm has disappeared. The intensity of CTB near 308 nm increases remarkably, whereas the excitation spectrum centered at 365 nm and related to the defect-induced band decreased drastically in Fig. 5(c) and (d). It is indicated that the relative emission intensity in $Sr_{2.35}Ba_{0.5}Sm_{0.1}Al_{0.9}In_{0.1}O_{4-\alpha}F_{1-\delta}$ under the excitation of 308 nm ($EM_{EX=308\ nm}$) was remarkably enhanced and rose to about 10 times that of the $Sr_{2.4985}Ba_{0.5}Sm_{0.001}Al_{0.9}In_{0.1}O_{4-\alpha}F_{1-\delta}$ as shown in Fig. 5(b) and (d). As a result, bright orange emitting $Sr_{2.5-3x/2}Ba_{0.5}Sm_xAl_{1-y}In_yO_{4-\alpha}F_{1-\delta}$ ($0.001\le x,\ y\le 0.1$) oxyfluoride phosphors under excitation light of at around 310 and 410 nm could be quite effective in producing white-emitting light for UV and near-UV LED applications.

4. Conclusions

Because of the replacement of Al^{3+} ions by In^{3+} ions in $Sr_{2.35}Ba_{0.5}Sm_{0.1}AlO_4F$, there was a gradual shift in the positions of the various Bragg reflections to lower angles. This substitution increased the local distortion of the Sm^{3+} ions as well as the covalency in the $Sr_{2.5-3x/2}Ba_{0.5}Sm_xAl_{1-y}In_yO_4F$ ($0.001\le x, y\le 0.1$) luminescent host lattice. A novel charge-transfer band centered at 304 nm shifted from 240 nm was observed in the photoluminescence spectra due to the cooperation of the InO_4 tetrahedra in the host lattice. Strong and well-resolved emitting peaks caused by crystal-field effects were monitored in $^4G_{5/2}\rightarrow{}^6H_J$ transitions of the Sm^{3+} activator in the oxyfluoride host lattice. The diverse excitation and emission spectra of $Sr_{2.5-3x/2}Ba_{0.5}Sm_xAl_{1-y}In_yO_{4-\alpha}F_{1-\delta}$ ($0.001\le x,\ y\le 0.1$) oxyfluoride phosphors originating from the CTB of O^{2-} to Sm^{3+} activator, the *f–f* transitions of the Sm^{3+} ions, and the defect-induced self-activated band were clearly monitored.

Acknowledgments

This research was supported by the Basic Science Research Program through the National Research Foundation of Korea (NRF) funded by the Ministry of Education, Science and Technology (2011-0010756). I would also like to express my gratitude for the support received from the SANHAKFUND 2010 Fellowship.

References

[1] E.F. Schubert, J.K. Kim, Science 308 (2005) 1274–1278.
[2] S. Ye, Y.X. Xiao, Y.X. Pan, Y.Y. Ma, Q.Y. Zhang, Mater. Sci. Eng. R 71 (2010) 1–34.
[3] J.S. Kim, P.E. Jeon, J.C. Choi, H.L. Park, S.I. Mho, G.C. Kim, Appl. Phys. Lett. 84 (2004) 2931–2933.
[4] W.J. Yang, T.M. Chen, Appl. Phys. Lett. 88 (2006) 101903.
[5] J. Zhang, L. Wang, Y. Jin, X. Zhang, Z. Hao, X.-J. Wang, J. Lumin. 131 (2011) 429–432.
[6] S. Sakirzanovas, A. Katelnikovas, H. Bettentrup, A. Kareiva, T. Jüstel, J. Lumin. 131 (2011) 1525–1529.
[7] S. Park, T. Vogt, J. Am. Chem. Soc. 132 (2010) 4516–4517.
[8] S. Park, T. Vogt, J. Phys. Chem. C 114 (2010) 11576–11583.
[9] S. Park, T. Vogt, J. Lumin. 129 (2009) 952–957.
[10] A.K. Prodjosantoso, B.J. Kennedy, T. Vogt, P.M. Woodward, J. Solid State Chem. 172 (2003) 89–94.
[11] S. Park, J. Lumin. 132 (2012) 875.
[12] R.D. Shannon, Acta Cryst. A 32 (1976) 751–767.
[13] L. Yang, X. Yu, S. Yang, C. Zhou, P. Zhou, W. Gao, P. Ye, Mater. Lett. 62 (2008) 907–910.
[14] Y. Tamura, A. Shibukawa, Jpn. J. Appl. Phys. 32 (1993) 3187–3196.
[15] W. Luo, R. Li, X. Chen, J. Phys. Chem. C 113 (2009) 8772–8777.